J Mater Sci (2011) 46:4487–4493
DOI 10.1007/s10853-011-5342-x

Pore size characteristics of nonwoven structures under uniaxial tensile loading

Amit Rawal · Sushil Kumar Agrahari

Received: 23 December 2010 / Accepted: 27 January 2011 / Published online: 10 February 2011

Abstract Nonwovens are highly porous structures consisting pores of complex shapes and sizes which are responsible for desired functional characteristics. In general, a nonwoven is often subjected to uniaxial tensile loading in various applications and it is of paramount importance to account for changes in structural characteristics including pore sizes during the loading conditions. In this research work, the pore size of thermally bonded nonwoven structures under uniaxial tensile loading at various levels of strains has been investigated. A theoretical model has been proposed that accounted for fibre reorientation and changes in the fibre volume fraction during the application of tensile strain. A comparison has been made between theoretical and experimental pore size distributions of thermally bonded nonwoven structures at defined levels of strains. Moreover, an attempt has been made to rationalise some of the contradictory literature results of pore size distributions of nonwoven structures under uniaxial tensile loading.

Introduction

Nonwovens are highly porous structures consisting pores of complex shapes and sizes. These complex pores are responsible for attaining certain functional characteristics in a nonwoven. Over the years, the range of nonwoven applications has become immeasurable due to their unique structural and functional characteristics. Therefore, these nonwoven structures are expected to perform more than one function for any engineering application. In these applications, it is easy to envisage a nonwoven being subjected to uniaxial tensile loading and accordingly changes in structural characteristics such as pore size, porosity, etc. need to be accounted. For example, a nonwoven scaffold is expected to have appropriate pore size for proper cell growth, proliferation and differentiation and simultaneously, the scaffold should be engineered to shield the nascent tissue from the mechanical stresses [1, 2]. A nonwoven acting as a separator squeezed between the fine soil and the coarse material is subjected to concentrated actions, i.e. perpendicular to the plane of the nonwoven geotextile leading to the tensile stresses in its plane [3]. In addition, the in-plane stresses and strains are also applied during the installation of a nonwoven that can significantly affect its performance for a desired application [4].

Numerous research papers have been published for understanding and predicting the pore size characteristics of stochastic fibrous assemblies such as nonwovens [5–8]. However, limited research work pertaining to the effect of in-plane tensile loading on pore size characteristics of nonwoven structures can be found in the literature [9–11]. More recently, Wu et al. [12] have studied the various levels of uniaxial tensile strain on the pore size characteristics of heat-bonded nonwoven geotextiles and woven slit films. However, the results obtained from the literature is found to be contradictory and in-conclusive as Fourie and Addis [10] have found that there is a decrease in the pore size of nonwoven structures under tensile loading whereas the opposite behaviour is observed in the research work of Wu et al. [12]. Moreover, the rationale for obtaining such results is also not clearly presented in the above research papers. Therefore, the main objective of this research work is to theoretically and experimentally determine the pore size distributions of thermally bonded nonwoven structures under uniaxial tensile loading at various levels of strains.

A. Rawal (✉) · S. K. Agrahari
Department of Textile Technology, Indian Institute of Technology Delhi, Hauz Khas, New Delhi, India
e-mail: arawal@textile.iitd.ac.in; amitrawal77@hotmail.com

It is our intention to rationalise some of the results given by Wu et al. [12] specifically in relation to the pore size of nonwoven structures under uniaxial tensile loading.

Theoretical

In the past, we have been able to successfully predict the pore size distribution of a monocomponent and hybrid[1]-based nonwoven structures using the principles of sieving-percolation pore network theory [13–15]. The pore network theory assumed that a nonwoven is a three-dimensional (3D) structure consisting of layers of fibres oriented in certain directions. This 3D model of nonwoven structure can be easily developed by assuming the fibres to be stacked in elementary longitudinal planes (i.e. parallel to the plane of sheet). It should be noted that there is no correlation between the orientations of fibres in these longitudinal planes. In this research work, we extend the previous pore model of hybrid nonwoven structures for uniaxial tensile loading condition [15]. Since, the pore model of hybrid nonwoven is more generalised in nature and can be used for a variety of nonwovens. In this model, the pore size of a nonwoven is assumed as a circle of defined diameter inscribed in a polygon formed by fibrous network and considering a combination of gamma distribution of polygon-inscribed circles along with a stereological approach accounting for the effect of fibre orientation [13]. Hence, the cumulative probability of a particle with diameter d, passing through the layers of nonwoven ($F_f(d)$) is shown below [15, 16].

$$F_{\mathrm{f}}(d) = 1 - \left[\left(1 + \omega d + \frac{\omega^2 d^2}{2}\right) e^{-\omega d}\right]^N \tag{1}$$

where

$$\omega = \frac{4 V_{\mathrm{f}} K_\alpha}{\pi \bar{D}} \tag{2}$$

$$K_\alpha = \int_{-\pi/2-\alpha}^{\pi/2-\alpha} |\cos \beta_{\mathrm{i}}| \chi(\beta_{\mathrm{i}}) d\beta_{\mathrm{i}} \tag{3}$$

$$N = \frac{T_{\mathrm{g}}}{\bar{D}} \tag{4}$$

and

$$\overline{D} = D_1 V_1^2 + (D_1 + D_2) V_1 V_2 + D_2 V_2^2 \tag{5}$$

where N is the number of layers, ω is the scale or coverage parameter, V_f is the total fibre volume fraction, $\chi(\beta_i)$ is the distribution function of initial fibre orientation angle (β_i), K_α is the directional parameter indicating when the average distance between the two bonds is projected on planar direction (α), d is the inscribed circle diameter, $\overline{D}$ is the probabilistic mean fibre diameter, D is the fibre diameter of defined fibre type, T_g is the nonwoven thickness, V is the fibre proportion and subscripts, 1 and 2 refer to fibre types present in a hybrid nonwoven.

Consider a fibre oriented at an initial orientation angle, β_i, with respect to the loading direction and reorientated to β_f under uniaxial tensile loading based on the affine deformation of fibre [17]. Therefore,

$$\beta_{\mathrm{f}} = \cos^{-1}\left[\frac{(1+\varepsilon)}{\sqrt{(1+\varepsilon)^2 + \tan^2 \beta_{\mathrm{i}} (1 - v\varepsilon)^2}}\right] \tag{6}$$

where v is the Poisson's ratio of the nonwoven with respect to the loading direction and the level of tensile strain (ε).

Hence, the directional parameter need to be updated based on the reorientation of fibres during the application of tensile loading. Thus, Eq. 3 has been modified to the following expression.

$$K_\alpha(\beta_{\mathrm{f}}) = \int_{-\pi/2-\alpha}^{\pi/2-\alpha} |\cos(\beta_{\mathrm{f}})| \chi(\beta_{\mathrm{f}}) d\beta_{\mathrm{f}} \tag{7}$$

Furthermore, there is relative change in the fabric volume during the application of uniaxial tensile loading and hence, the fibre volume fraction needs to be updated as derived by Giroud [18].

$$V_{\mathrm{f}}(\varepsilon) = \frac{V_{\mathrm{f}}}{(1+\varepsilon)(1-v\varepsilon)^2} \tag{8}$$

Also,

$$V_{\mathrm{f}} = \frac{\mu}{T_{\mathrm{g}} \rho_{\mathrm{h}}} \tag{9}$$

and

$$\rho_{\mathrm{h}} = \frac{\rho_1 \rho_2}{x \rho_2 + (1-x) \rho_1} \tag{10}$$

where μ is the mass per unit area of nonwoven, T_g is the nonwoven thickness, x is the weight fraction or proportion of fibres in a hybrid nonwoven, ρ is the density of fibres (subscripts 1 or 2 refer to fibre types) and ρ_h is the equivalent fibre density.

A Matlab® programme was written to calculate the pore size distribution of hybrid nonwoven structures at defined levels of strains by combining the Eqs. 1–10.

Experimental

The reported study is based on two thermally bonded nonwoven structures, produced and supplied by the company, i.e. Libeltex in the previous research work [19, 20].

[1] Hybrid term refers to the material consisting of two types of fibres.

These structures were produced by blending the homofil and bicomponent (core-sheath) polyester fibres in equal proportions by weight and labelled here as TB1 and TB2. The basic difference between the above nonwovens is that the finer and the coarser fibres have been used in the TB1 and TB2, respectively as illustrated in Fig. 1. Some of the important constituent fibre properties are given in Table 1. The nominal mass per unit area of both nonwovens is 30 g/m^2 and the thickness of TB1 and TB2 were found to be 0.44 and 0.43 mm, respectively at a pressure of 0.69 kPa. The stress–strain curves of these nonwovens were determined by cutting the fabric strips of 20 × 15 cm and tested on an Instron tensile testing machine under uniaxial loading at a strain rate of 10 mm/min. Figure 2 shows a comparison between the stress–strain curves of thermally bonded nonwoven structures. In-plane fibre orientation distributions of thermally bonded nonwoven structures have also been determined and reported earlier [17]. Furthermore, the Poisson's ratio of nonwoven structures was determined at defined strain levels of 4, 8 and 12% using Messphysik® videoextensometer. The videoextensometer works on the principle of evaluation of the grey contrast between the specimen surface and the markers. The details of the above measurement technique can be obtained in Rawal et al. [20]. Table 2 presents the Poisson's ratio values in both machine and cross-machine directions at defined levels of strains. Pore size is measured in the unstrained samples of nonwoven structures using image analysis software (Leica Qwin®) by fitting the circles of *maximum* diameter formed between the polygonal networks of constituent fibres, as shown in Fig. 3. In case of strained nonwovens, two glass slides were glued on the sample using a commercial adhesive (Quickfix®) *whilst* it is kept under strained condition on the tensile testing machine. The samples were kept for an average of 5 h such that the adhesive can set well and no further relaxation of nonwoven can take place after being removed from the tensile testing machine. Subsequently, the region consisting of glass slides was cut free from the remaining sample and a procedure to measure the pore size of a nonwoven was followed as that of unstrained sample.

Table 1 Fibre types used in the production of thermally bonded nonwoven structures

Fibre parameters		TB1	TB2
Fibre length (mm)	Homofil	48.83	47.80
	Bicomponent	58.38	61.22
Linear density (dtex)	Homofil	3.3	12
	Bicomponent	2.2	4.4
Diameter (μm)	Homofil	18.30	34.90
	Bicomponent	14.90	21.10
Density (g/cm^3)		1.38	1.38
Melting temperature of homofil fibre (°C)		250	250
Melting temperature of sheath in bicomponent fibre (°C)		110	110

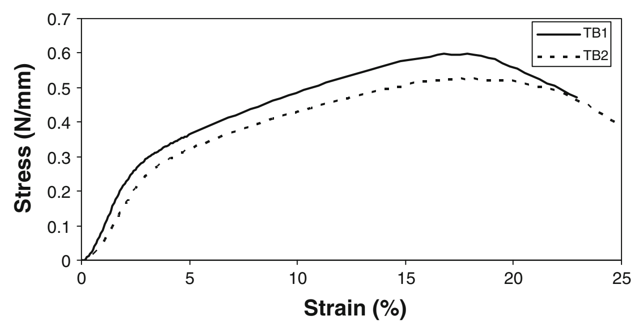

Fig. 2 Stress–strain curves of thermally bonded nonwoven structures

Table 2 Poisson's ratio of TB1 and TB2 under defined strain levels

Strain (%)	TB1 (MD)	TB1 (CD)	TB2 (MD)	TB2 (CD)
4	2.90	0.71	3.81	0.51
8	2.64	0.75	2.92	0.50
12	2.38	0.83	2.61	0.51

MD machine direction, *CD* cross-machine direction

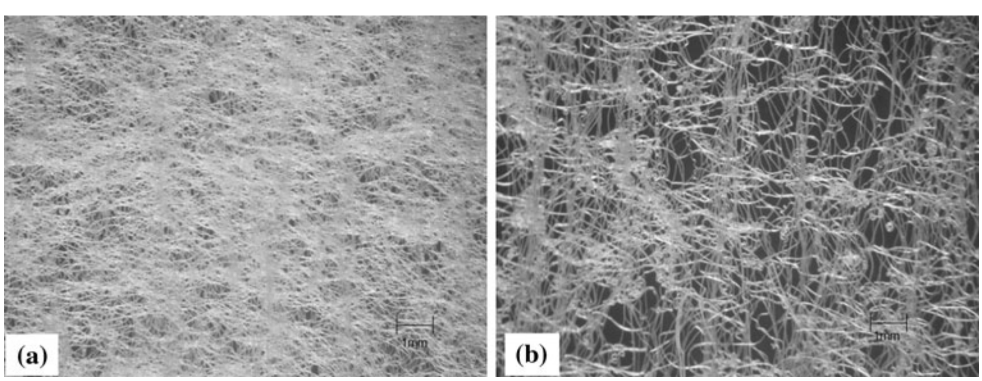

Fig. 1 Images of **a** TB1 and **b** TB2 nonwoven structures, *scale bar* 1 mm

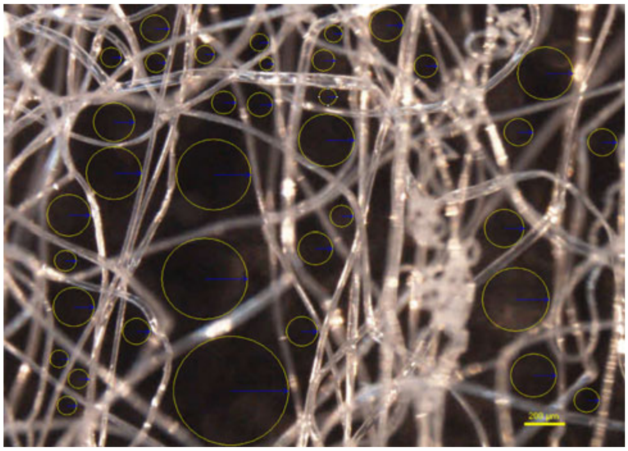

Fig. 3 Measurement of pore size as circles of *maximum* diameter fitted in the polygonal network of fibres, *scale bar* 200 µm

Results and discussion

TB1 has pores of smaller sizes in comparison to TB2 that has coarser constituent fibres as illustrated in Fig. 4 and it is also evident from micrographs (shown in Fig. 1) that a dense assembly of fibres is observed in various regions of TB1. In general, there is a decrease in the pore size of thermally bonded nonwoven structures with the applied tensile strain, as shown in Fig. 5. For example, O_{98} (defined as the particle diameter at which 98% by weight is retained on the nonwoven) values decrease with an increase in the longitudinal strain, as shown in Table 3. It must be noted that these pore sizes are measured in the machine direction and the directional parameter values computed using Eq. 3 for TB1 and TB2 is found to be 0.81 and 0.77, respectively under unstrained state [20]. The value of directional parameter (K_{α}) for randomly isotropic distributed fibres is 0.63. We will discuss later about the importance of the machine direction in determining the pore sizes at defined levels of tensile strains.

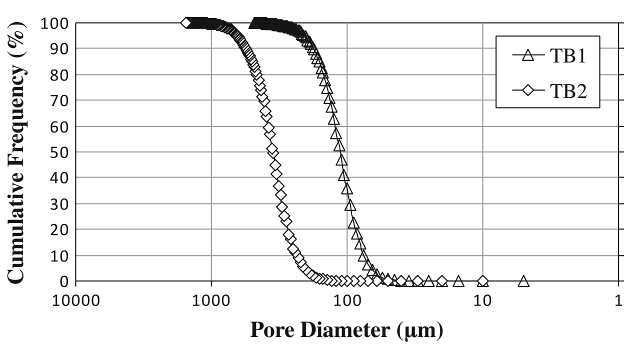

Fig. 4 Comparison of pore size distributions for thermally bonded nonwoven structures, TB1 and TB2

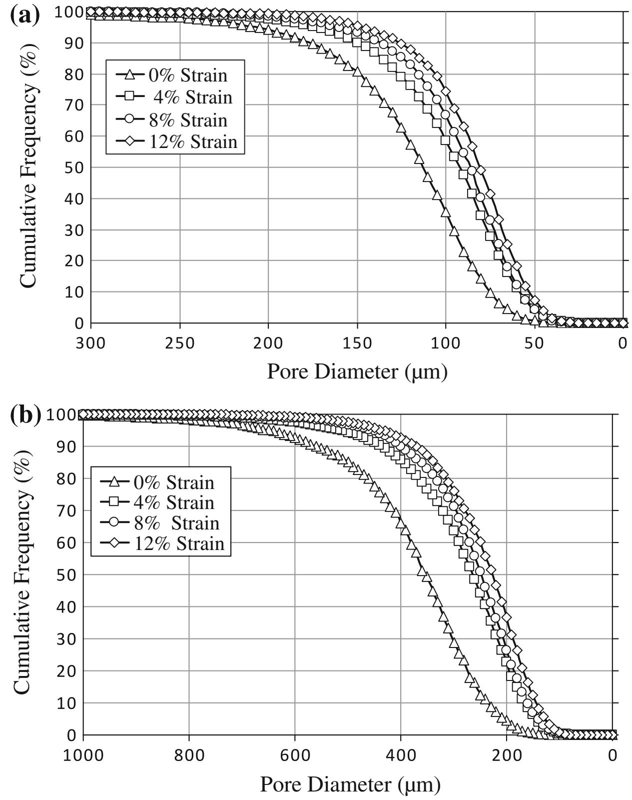

Fig. 5 Pore size distribution as a function of tensile strain in **a** TB1, **b** TB2 nonwovens

Table 3 O_{98} (µm) values of TB1 and TB2 under defined strain levels

Strain (%)	TB1	TB2
0	250	770
4	210	640
8	195	550
12	175	520

Comparison between theoretical and experimental results

The pore size distributions of thermally bonded nonwoven structures have been theoretically calculated using Eqs. 1–10 and subsequently, a comparison has been made between the theoretical and experimental results. In general, a good agreement has been found between the theoretical and experimental results of pore size distribution with the applied strain, as shown in Figs 6 and 7. The small differences between two sets of results are due to the fact that the tensile test is assumed to be a 'perfect' uniaxial test which may not be the case in reality [18]. Since, it is well-known that the lateral strain is non-uniform over the entire length of the specimen.

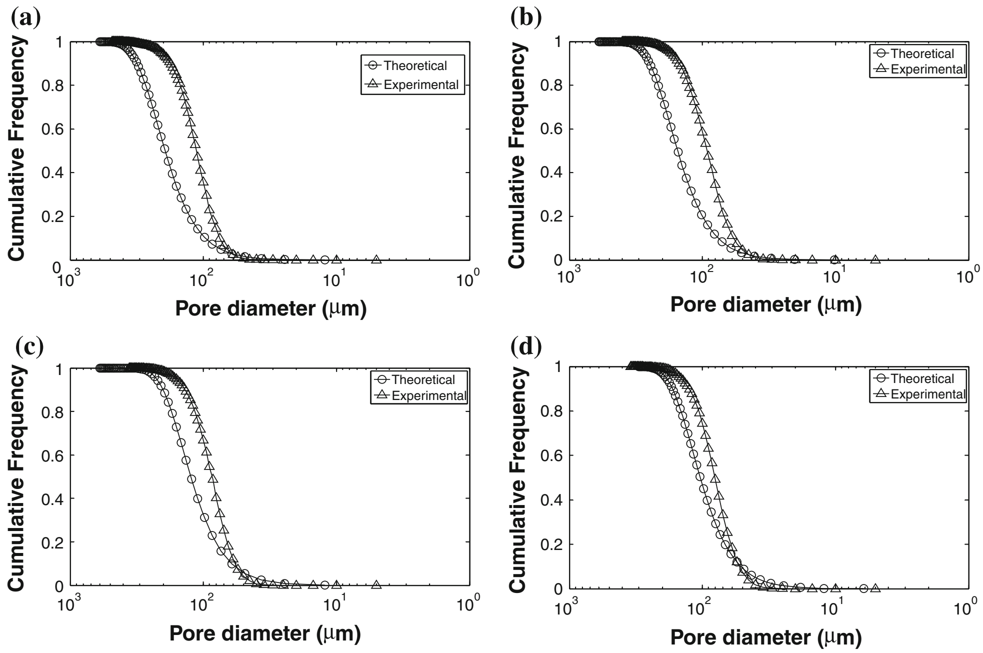

Fig. 6 Comparison between theoretical and experimental pore size distributions of TB1 under **a** 0%, **b** 4%, **c** 8%, and **d** 12% strain

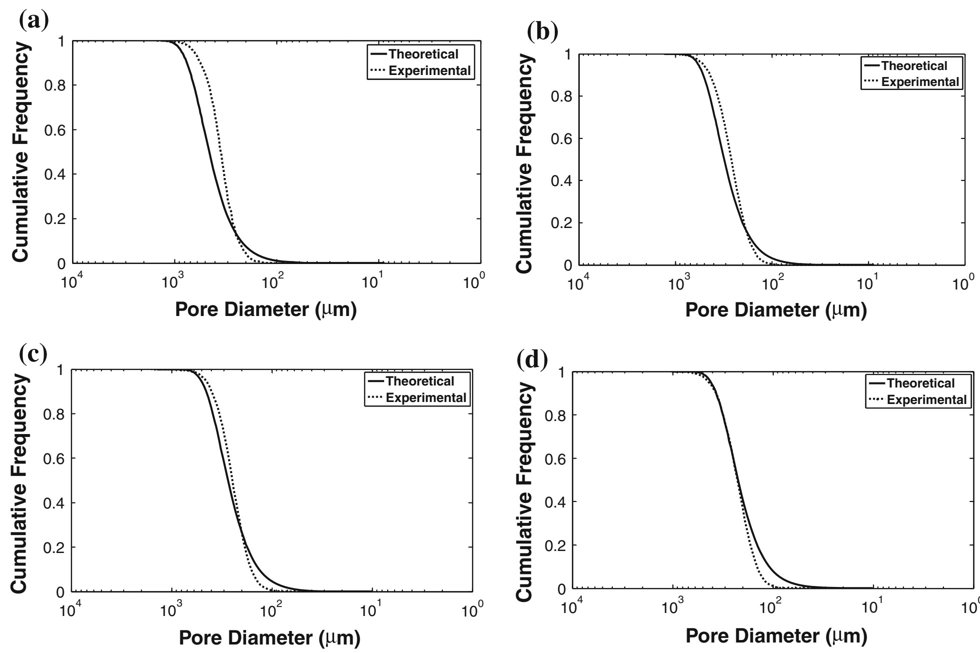

Fig. 7 Comparison between theoretical and experimental pore size distributions of TB2 under **a** 0%, **b** 4%, **c** 8%, and **d** 12% strain

Rationalisation of literature results of pore size distribution of nonwovens under uniaxial tensile loading

According to Fourie and Addis [10], the pore size of nonwoven structures decreases with an increase in uniaxial tensile strain. On the other hand, Wu et al. [12] have shown the contrary trend of pore size distribution of thermally bonded nonwovens under uniaxial tensile loading. This clearly shows that there is a high level of ambiguity existing between these results. In general, nonwoven structures are anisotropic in nature and most of them are preferentially orientated, i.e. majority of fibres/filaments are aligned around one direction. When a uniaxial tensile loading is applied in the preferential direction, significant amount of fibre reorientation occurs, leading to high degree

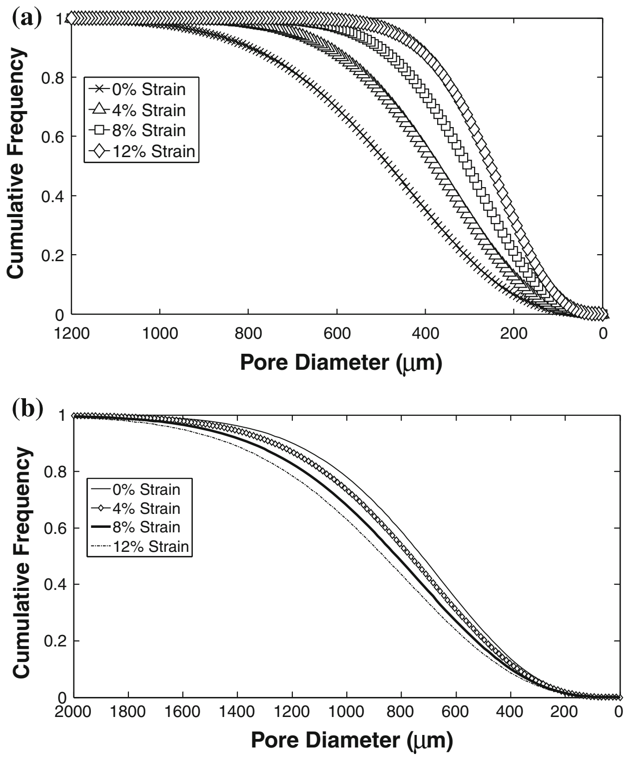

Fig. 8 Theoretical pore size distributions of TB2 at various levels of strains in **a** machine direction, **b** cross-machine direction

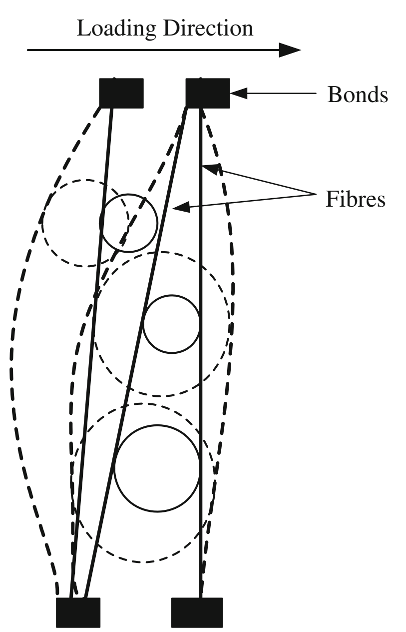

Fig. 9 Shearing of fibres in nonwoven structures. Here *solid* and *dotted lines* represent initial and final state of fibres before and after uniaxial tensile loading, respectively

of lateral contraction in the nonwoven structure. This reorientation of fibres would decrease the space between them and the fibre volume fraction is expected to increase with the uniaxial tensile strain. We demonstrate this phenomenon by predicting the pore size distributions of preferentially orientated nonwoven, TB2, in the machine direction, as shown in Fig. 8a. However, when the pore size is predicted in the cross-machine direction for the same nonwoven, the opposite trend can be observed (see Fig. 8b). This may be due to the fact that the majority of the fibres aligned in the preferential direction would tend to experience shear forces *whilst* moving towards the applied direction resulting in bending of fibres forming pores of relatively larger size corresponding to the unstrained positions, as shown in Fig. 9. Surprisingly, Wu et al. [12] neither determined the fibre orientation distribution nor the direction of measurement for pore size distribution was explicitly stated in their results. Therefore, we believe that the test direction has a significant role to play in determining the pore size distribution of a nonwoven structure.

Conclusions

In this research work, the existing model of pore size distribution for *hybrid* nonwoven structures based on sieving-percolation pore network theory has been modified by accounting for uniaxial tensile loading condition. In general, a good agreement has been observed between the theoretical and experimental results of pore size distribution of thermally bonded nonwovens under defined levels of tensile strains. In general, it was found that there is a decrease in the pore size of thermally bonded nonwoven structure in the machine direction with an increase in tensile strain. However, the pore size of a nonwoven can increase with the application of tensile strain when the former is analysed in the cross-machine direction owing to the fact that it is a preferentially orientated type of structure. Therefore, it is utmost important for a nonwoven designer to account for the direction of placement of nonwoven structure and quantify its anisotropic characteristics specifically for pore related applications. In future, the sensitivity of pore size distributions needs to be analysed by means of first and second moments.

Acknowledgements AR wishes to express the gratitude to DST, India for financially supporting this research work. This study has been supported by DST, India under ‘Fast Track Scheme for Young Scientists’ programme.

References

1. Li Y, Ma T, Yang ST, Kniss DA (2001) Biomaterials 22:609
2. Engelmayr GC, Sacks MS (2006) J Biomech Eng 128:610
3. Giroud JP (1981) Mater Constr 14:257
4. Hufenus R, Rüegger R, Flum D, Sterba IJ (2005) Geotext Geomembr 23:401

5. Ogston AG (1958) Trans Faraday Soc 54:1754
6. Dodson CTJ, Sampson WW (1999) J Stat Phys 96:447
7. Bosma C, Wesselingh JA (2000) J Chromatogr B 743:169
8. Chatterjee AP (2010) J Appl Phys 108:063513
9. Fourie AB, Kuchena SM (1995) Geosynth Int 2:455
10. Fourie AB, Addis PC (1997) Geotech Test J 20:211
11. Fourie AB, Addis PC (1999) Geotext Geomembr 17:331
12. Wu CS, Hong YS, Wang RH (2008) Geotext Geomembr 26:250
13. Rawal A (2010) J Text Inst 101:350
14. Rawal A, Kameswara Rao PV, Russell S, Jeganathan A (2010) J Appl Polym Sci 118:2668
15. Rawal A and Saraswat H. Geotext Geomembr. doi:10.1016/j.geotexmem.2010.12.006
16. Pan N, Chen J, Seo M, Backer S (1997) Text Res J 67:907
17. Rawal A, Priyadarshi A, Lomov SV, Verpoest I, Vankerrebrouck J (2010) J Mater Sci 45:2274. doi:10.1007/s10853-009-4152-x
18. Giroud JP (2004) Geotext Geomembr 22:297
19. Rawal A, Lomov SV, Ngo T, Verpoest I, Vankerrebrouck J (2007) Text Res J 77:417
20. Rawal A, Priyadarshi A, Kumar N, Lomov SV, Verpoest I (2010) J Mater Sci 45:6643. doi:10.1007/s10853-010-4755-2